QSAR Analysis of Δ^8-THC Analogues: Relationship of Side-Chain Conformation to Cannabinoid Receptor Affinity and Pharmacological Potency

Alison R. Keimowitz,[†] Billy R. Martin,[§] Raj K. Razdan,[‡] Peter J. Crocker,[‡] S. Wayne Mascarella,[†] and Brian F. Thomas*[,†]

Research Triangle Institute, P.O. Box 12194, Research Triangle Park, North Carolina 27709-2194, Department of Pharmacology and Toxicology, MCV/VCU, Richmond, Virginia 23298, and Organix Inc., 240 Salem Street, Woburn, Massachusetts 01801

Received May 7, 1999

A novel quantitative structure−activity relationship (QSAR) for the side-chain region of Δ^8-tetrahydrocannabinol (Δ^8-THC) analogues is reported. A series of 36 side-chain-substituted Δ^8-THCs with a wide range of pharmacological potency and CB1 receptor affinity was investigated using computational molecular modeling and QSAR analyses. The conformational mobility of each compound's side chain was characterized using a quenched molecular dynamics approach. The QSAR techniques included a modified active analogue approach (MAA), multiple linear regression analyses (MLR), and comparative molecular field analysis (CoMFA) studies. All three approaches yielded consistent results. The MAA approach applied to a set of alkene/alkyne pairs identified the most active conformers as those with conformational mobility constrained within an approximately 8 Å radius. MLR analyses (restricted to 15 hydrocarbon side-chain analogues) identified two variables describing side-chain length and terminus position that were able to fit the pharmacological data for receptor affinity with a correlation coefficient for pK_D of 0.82. While chain length was found to be directly related to receptor affinity, the angle made by the side chain from its attachment point to its terminus (angle defined by C3−C1′−side-chain terminus carbon, see Figure 1) was found to be inversely related to affinity. These results suggest that increased side-chain length and increased side-chain ability to wrap around the ring system are predicted to increase affinity. Therefore, the side chain's conformational mobility must not restrict the chain straight away from the ring system but must allow the chain to wrap back around toward the ring system. Finally, the CoMFA analyses involved all 36 analogues; they also provided data to support the hypothesis that for optimum affinity and potency the side chain must have conformational freedom that allows its terminus to fold back and come into proximity with the phenolic ring.

Introduction

Two cannabinoid receptors have been identified: the predominantly neuronal CB1 receptor[1] and the predominantly peripheral CB2 receptor.[2] It has been shown that these receptors are G-protein linked and that cannabinoids act to modulate adenyl cyclase[3,4] and Ca^{2+} and K^+ currents.[5−7] Through their interaction with these receptors, cannabinoids produce "cannabimimetic" effects in animals, including antinociception, hypothermia, hypomotility, and catalepsy in mice.[8] These effects, which have been shown to be correlated to pyschoactivity in humans,[9] can be blocked by SR141716A and other cannabinoid receptor antagonists.[10,11]

A variety of structural classes can interact with CB1 or CB2, including classical and nonclassical cannabinoids,[12] aminoalkylindoles,[13] benzofurans,[14] fatty acid ethanolamides,[15] and pyrazoles.[16] Unfortunately, no direct observation of a cannabinoid bound to a cannabinoid receptor using X-ray crystallography has been reported. Thus, pharmacophoric elements of a ligand's interaction with these receptors have been inferred from many approaches, such as receptor binding analyses of a variety of cannabinoid analogues using wild-type and mutated receptor systems[17] and also through the use of computer-aided molecular modeling techniques.[18−26]

Molecular modeling studies and SAR analyses have indicated a number of regions in the classical cannabinoid structure which are important in determining receptor affinity and pharmacological potency such as the phenolic hydroxyl at C1,[21] the C9 position,[19,27] and the side chain.[23] Indeed, the cannabinoid side chain, which is the focus of this study, has been known to be a key pharmacophore since Adams demonstrated the increased potency of the dimethylheptyl analogue of Δ^{6a-10a}-THC.[28] More recent studies have further demonstrated the critical role played by side-chain length and conformation in determining pharmacological activity (see refs 27, 29−31 for examples). For example, in studies by Martin et al.[32] the substitution of the pentyl side chain of the inactive cannabinoid 11-nor,9-COOH-Δ^9-THC with a dimethylheptyl side chain resulted in an active compound, approximately equipotent to Δ^9-THC itself. Finally, constrained side-chain analogues have provided some additional information regarding the side-chain region of cannabinoids[31,33] and its relationship to determining pharmacological activity.

Despite the recognition of the aliphatic side chain as being a key pharmacophoric element in cannabinoids, the bioactive conformation(s) of the side chain has never

* Corresponding author. E-mail: bft@rti.org.
[†] Research Triangle Institute.
[§] MCV/VCU.
[‡] Organix Inc.

10.1021/jm9902281 CCC: $19.00
Published on Web 12/10/1999

been clearly elucidated. QSAR studies of classical cannabinoids have typically been performed on single side-chain conformations that have been obtained by procedures that minimize the total molecule's energy.[34] Studies have also been performed on conformers selected by procedures that find energy minima for specific regions or bonds. For example, cannabinoids assumed to have all syn alignments along the bonds of the side chain, thus minimizing the energy at each bond, have been studied.[35] It is unclear how these low-energy conformers are related to the bioactive conformer, however, because of the many alternative conformations that may be assumed by conformationally flexible side chains in biological matrixes or during ligand−receptor interaction. Indeed, it has been shown for small flexible molecules that the protein-bound and crystal conformations are energetically well above the global minimum and, in many instances, not even in any local energy minimum.[36]

In this study, the problem of selecting hypothetical bioactive conformers was bypassed because a conformational ensemble for each analogue was generated using molecular dynamics simulations and subsequently used in each QSAR approach. This builds on previous studies which have utilized the multiplicity of conformers generated by molecular dynamics to determine and compare conformationally accessible regions.[24]

These ensembles were analyzed with SAR and QSAR techniques to detect differences in conformations or conformationally accessible regions that can explain differences in receptor affinity and pharmacological potency for each cannabinoid analogue. The SAR analyses allowed the identification and visualization of a three-dimensional pharmacophoric requirement for the entire side-chain region. The results of this study should aide in the design and synthesis of rigid or constrained side-chain analogues and facilitate further elucidation of this critical region of the cannabinoid pharmacophore.

Methods

Molecular Modeling. Molecules were modeled using SYBYL (Tripos Inc., St. Louis, MO), and electrostatic charges of each compound were calculated with the Gasteiger−Hückle method. Each compound was energy minimized using the SYBYL force field with a conjugate gradient of 0.001 kcal/mol or a maximum of 100 000 iterations as termination criteria.

Quenched Molecular Dynamics. Molecular dynamics were computed for each energy-minimized structure at temperatures from 100 to 1000 K. At each 100 K step, the molecule was allowed to remain at the specified temperature for 1 ps while snapshots of the conformation were acquired every 200 fs. Upon reaching 1000 K, the molecule was held at this temperature for 100 ps while snapshots were acquired at 1-ps intervals. This procedure yielded a total of 155 snapshots of different conformers for each molecule investigated. The Gasteiger−Hückel charges were taken into consideration throughout this molecular dynamics procedure. Every conformation obtained for a particular molecule was then energy minimized again using a less stringent conjugate gradient of 0.01 kcal/mol or a maximum of 100 000 iterations as termination criteria, yielding a group of 155 energy-minimized conformers per compound.

Molecular and Conformational Alignment. One conformation of one compound (3-(3-octynyl)-Δ^8-THC, **5**) was used as a template molecule; it was unimportant which molecule was used for this template, so long as it was applied consistently, because the phenyl ring systems of all analogues were identical. All conformations of all compounds were aligned in space so as to overlay as closely as possible the six aromatic carbons of their phenol ring system with the corresponding atoms in the template molecule. The alignment was performed using atom-by-atom root-mean-square distance minimization. This alignment positions all of the molecules in the same three-dimensional space and superposes the ring systems to as great an extent as possible; since the side chains are not part of the alignment rule, this feature of the molecule could be compared between conformers of the same compound as well as between different compounds using the QSAR techniques described below.

Quantitative Structure−Activity Analyses. Three approaches to QSAR analysis were applied to the compounds listed in Table 1. The biological data used as the target values for these structure−activity analyses included CB1 receptor binding affinity (Table 1) and pharmacological potency (ED_{50}'s) in three assays associated with cannabimimetic activity.[37] This reference contains the full pharmacological data (K_D, as derived from K_i, and ED_{50}'s for the spontaneous activity, tail-flick, and rectal temperature assays) as well as the methods used to determine it. This full data set is also available as Supporting Information.

Active Analogue Approach on Alkene/Alkyne Side-Chain Analogues of Δ^8-THC. The first study used a modified "active analogue" approach and was restricted to alkene and alkyne pairs. This subset of compounds included the following pairs of C3-substituted analogues of Δ^8-THC (see Table 1): 1-heptynyl and *cis*-1-heptenyl, 2-octynyl and *cis*-2-octenyl, 3-octynyl and *cis*-3-octenyl, 4-octynyl and *cis*-4-octenyl, 6-bromo-2-hexynyl and *cis*-6-bromo-2-hexenyl, which differ from one another only by the bond order at a single position in the side chain. Each alkene/alkyne pair had one compound described as active and one described as less active. The alkenes were "active" with ED_{50}'s for various rat behavioral assays ranging from 0.05 to 0.57 mg/kg, whereas the "less active" alkynes' ED_{50}'s ranged from 0.51 to 29 mg/kg. The differences in ED_{50}'s for any behavioral assay within an alkene/alkyne pair ranged from 0.49 to 28.05 mg/kg. Note that those compounds designated "less active" are not fully inactive but rather are relatively inactive as compared to those compounds designated "active" and could therefore be treated as inactive in the context of this approach.

For each analogue, the 155 energy-minimized conformers were overlaid and the union of their molecular volume was calculated to obtain an approximation of the "conformationally accessible volume" for each compound. These "conformationally accessible volumes" were used to determine whether a relationship exists between molecular volume and potency via a method similar to that described by Marshall et al.[38] Initially, the volume not occupied by the receptor was overestimated by the union of the volume of the fully efficacious or "active" compounds. If RUA is this receptor unoccupied area, then

$$RUA = \bigcup_{n=1}^{5} A_n$$

where A_n is the combined molecular volume of all conformers of each (nth) active compound.

The area that is not occupied by any conformations of active analogues but is occupied by conformations of less active compounds was found through subtraction of the intersection of the conformationally accessible volumes of all compounds from the union of the conformationally accessible volumes of the less active compounds. This active-excluded area (AEA) can be thought of as an overestimate of the receptor essential volume (REV)[38] and is obtained as follows:

$$AEA = \bigcup_{n=1}^{5} I_n - \left[\bigcap_{n=1}^{5} A_n \bigcap_{n=1}^{5} I_n\right]$$

where I_n is the combined molecular volume of all conformers of the nth "less active" compound. Finally, a region that is

Table 1. Structure and CB1 Receptor Affinity of Δ⁸-THC Side-Chain Analogues

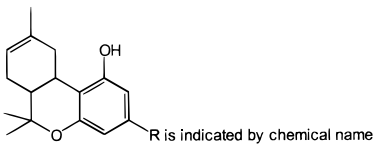

analyses[a]	compd	chemical name	K_D (nM)
a,m,s	**1**	3-(1-heptynyl)-Δ⁸-THC	36 ± 0.8
a,m,s	**2**	*cis*-3-(1-heptenyl)-Δ⁸-THC	0.86 ± 0.09
a,m,s	**3**	3-(2-octynyl)-Δ⁸-THC	4.9 ± 2.0
a,m,s	**4**	*cis*-3-(2-octenyl)-Δ⁸-THC	3.19 ± 0.92
a,m,s	**5**	3-(3-octynyl)-Δ⁸-THC	9.0 ± 1.3
a,m,s	**6**	*cis*-3-(3-octenyl)-Δ⁸-THC	3.36 ± 0.91
a,m,s	**7**	3-(4-octynyl)-Δ⁸-THC	19 ± 1.3
a,m,s	**8**	*cis*-3-(4-octenyl)-Δ⁸-THC	11 ± 3.2
a,s	**9**	3-(6-bromo-2-hexynyl)-Δ⁸-THC	1.2 ± 0.1
a,s	**10**	*cis*-3-(6-bromo-2-hexenyl)-Δ⁸-THC	1.66 ± 0.66
m,s	**11**	*O*-methyl-3-(2-octynyl)-Δ⁸-THC	189 ± 20
m,s	**12**	3-(2-hexynyl)-Δ⁸-THC	11 ± 1.0
m,s	**13**	3-(2-nonynyl)-Δ⁸-THC	3.7 ± 1.3
m,s	**14**	3-(3-butynyl)-Δ⁸-THC	367 ± 23
m,s	**15**	3-(1,6-heptadiynyl)-Δ⁸ -THC	460 ± 79
m,s	**16**	Δ⁸-THC	45 ± 12
m,s	**17**	3-(2,7-octadiynyl)-Δ⁸-THC	4.7 ± 0.4
s	**18**	3-(5-cyano-1-pentynyl)-Δ⁸-THC	104 ± 12
s	**19**	3-(3-carbomethoxy-2-propynyl)-Δ⁸-THC	731 ± 139
s	**20**	3-(4-bromo-2-butynyl)-Δ⁸-THC	143 ± 31
s	**21**	3-(4-bromo-2-pentynyl)-Δ⁸-THC	25 ± 2.5
s	**22**	3-(5-hydroxy-2-pentynyl)-Δ⁸-THC	448 ± 75
s	**23**	3-(5-cyano-2-pentynyl)-Δ⁸-THC	31 ± 8.3
s	**24**	3-(5-acetamido-2-pentynyl)-Δ⁸-THC	307 ± 24
s	**25**	3-(6-nitro-2-hexynyl)-Δ⁸-THC	5.34 ± 0.75
s	**26**	3-(4-carbomethoxy-3-butynyl)-Δ⁸-THC	>10000
s	**27**	3-(6-carboxy-1,2-hexadienyl)-Δ⁸-THC	3170 ± 105
s	**28**	3-(6-amino-2-hexynyl)-Δ⁸-THC	1300 ± 180
s	**29**	3-(6-cyano-2-hexenyl)-Δ⁸-THC	0.77 ± 0.05
s	**30**	*cis*-3-(6-cyano-2-hexenyl)-Δ⁸-THC	1.25 ± 0.51
s	**31**	*cis*-3-(6-fluoro-2-hexenyl)-Δ⁸-THC	20.9 ± 1.91
s	**32**	*cis*-3-(6-hydroxy-2-hexenyl)-Δ⁸-THC	53.7 ± 6.5
s	**33**	*cis*-3-(6-methoxy-2-hexenyl)-Δ⁸-THC	11.5 ± 0.16
s	**34**	*cis*-3-(6-acetamido-2-hexenyl)-Δ⁸-THC	16.7 ± 1.51
s	**35**	*cis*-3-(7-nitro-2-heptenyl)-Δ⁸-THC	3.56 ± 2.18
s	**36**	3-(1′,1′-dimethylheptyl)-Δ⁸-THC	0.77 ± 0.12

[a] The analyses column denotes in which QSAR analyses each compound was tested: a = active analogue approach, m = multiple linear regression, s = SAR/PLS CoMFA analysis.

necessary but not sufficient for activity was found by subtraction of the intersection of all compounds' volumes from the intersection of active conformers' volumes. If NR is this necessary region, then

$$NR = \bigcap_{n=1}^{5} A_n - \bigcap_{n=1}^{5} A_n \bigcap_{n=1}^{5} I_n$$

MLR Analysis of Hydrocarbon Side-Chain Analogues. The second study was restricted to compounds with side chains containing only hydrogen and carbon and used a multiple linear regression analysis as a means of identifying SAR. The

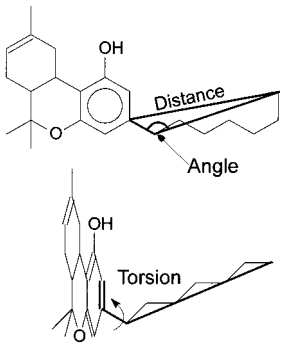

Figure 1. Descriptive variables used in MLR analyses of side-chain analogues of Δ⁸-THC.

compounds used were the following side-chain-substituted analogues of Δ⁸-THC: 1-heptynyl, *cis*-1-heptenyl, 2-octynyl, *cis*-2-octenyl, 3-octynyl, *cis*-3-octenyl, 4-octynyl, *cis*-4-octenyl, *O*-methyl-2-octynyl, 2-hexynyl, 2-nonynyl, 3-butynyl, 1,6-heptadiynyl, 2,7-octadiynyl, and Δ⁸-THC itself (see Table 1). In this "hydrocarbon" subset, intercompound differences in the electrostatic properties of the side chains were minimized by the exclusion of heteroatom and halogen atom substitution. The negative logs of the pharmacological data from three behavioral assays were used as the dependent variables in these analyses. These variables were: pK_D, negative log of the K_D at the CB1 receptor; pED$_{50}$_RT, negative log of the ED$_{50}$ in the mouse hypothermia assay; pED$_{50}$_SA, negative log of the ED$_{50}$ in the mouse spontaneous activity assay; and pED$_{50}$_TF, negative log of the ED$_{50}$ in the mouse tail-flick assay of antinociception (for full data, see ref 37).

The three independent variables were obtained according to the molecules' geometry (Figure 1). **Distance** was defined as the distance through space (not along bonds) between the point of attachment of the alkyl side chain and the end of the chain. The **angle** was defined by the phenyl ring's side-chain attachment point carbon, the first carbon of the side chain, and the terminal non-hydrogen atom of the side chain. The **torsion angle** was defined as the angle the terminus of the side chain made with the phenyl plane as a whole. These three variables localized the side chain of each conformation in three-dimensional space. To extend these molecular descriptors of the side chain of each conformation to a description of the overall conformational preference of the compound, the Boltzmann weighted average distance, angle, and torsion angle were calculated for each conformational ensemble using the following Boltzmann weighting factor (WF):

$$WF = e^{-[(E_c - E_{min})]/RT}$$

where E_c is the energy of the conformer, E_{min} is the minimum energy of any conformer of that compound, R is the gas law constant, and T is the temperature in Kelvin, always assumed to be 298. A variety of multivariate regressions were performed to seek correlations between the Boltzmann weighted average distance, torsion angle, and/or angle and the compounds' affinities and pharmacological potencies.

CoMFA of the Entire Set of Side-Chain Analogues. The third analysis was based on CoMFA and involved all of the compounds shown in Table 1. This technique has been previously used successfully in QSAR studies of cannabinoids.[22,24,25,35] In this method the descriptive variables were steric and electrostatic descriptions of the three-dimensional structure of the entire set of compounds. The CoMFA analysis was performed using a proton (H^{1+}) probe atom positioned at lattice points spaced around the molecules at 2 Å increments. Cross-validation was performed by randomly selecting 80% of the compounds to form a training set, developing a QSAR model based on their three-dimensional steric and electrostatic properties, and using this model to predict the dependent variables of the remaining 20% of the compounds that were not included in the training set. The predicted dependent

Table 2. MLR Analysis of the Relationship between Side-Chain Descriptors and Pharmacological Activity

Boltzmann weighted side-chain descriptors used as independent variables	dependent variable	r^2	r^2 adj[a]	prob > F	n
distance	pK_D	0.672	0.618	0.001	15
angle				0.002	
distance	pRT	0.418	0.321	0.017	15
angle				0.071	
distance	pTF	0.575	0.504	0.004	15
angle				0.008	
distance	pSA	0.380	0.277	0.030	15
angle				0.064	

[a] An r^2 adj of >0.5 is generally considered significant. The value for pTF was not considered significant, as it was so close to this cutoff.

variable of the compounds that were omitted from the training set was then compared against the actual dependent variable (e.g. receptor affinity) and a correlation coefficient obtained. This process was repeated randomly until every compound had been omitted from the training set and had its dependent variables predicted at least once. The correlation coefficients of the entire process were tracked throughout this process and the average r^2 values were calculated as a measure of the press, or the robustness, of the model.

It was not possible to analyze all 155 conformers per molecule, e.g. 5580 total conformers, because the size of the molecular spreadsheet and its manipulation became intractable. A number of different statistical sampling techniques were used to select conformers to analyze, see Table 3. Technique 1 was to take 50 random conformations from the 155 total and treat them as a representative sample. Technique 2 was to take 10 random conformations from the 155 total and treat them as a representative sample. Technique 3 analyzed the 20 overall lowest-energy conformers for each compound. In technique 4 the results of technique 2 were used. For each compound, the 10 lowest-energy conformers from the 50 random conformers previously analyzed in technique 1 were selected; this 360 conformer data set was then analyzed. Technique 5 examined the one lowest-energy conformer of each compound. Control studies were also run where randomized pharmacological data was used in place of real pharmacological data. These artificial points were random numbers generated to fall within the range of the real data. The same cross-validated and final analyses were performed in the control studies to check that the r^2 values were higher when pharmacological data were used than when artificial data were used.

Results

Quenched Molecular Dynamics. The quenched molecular dynamics approach used for conformational sampling generated 155 low-energy conformations for each molecule. The conformations were quite diverse for certain molecules, while other molecules repeatedly yielded a small number of similar conformations. These differences in conformational mobility can be visualized graphically by overlaying the conformations for a particular molecule or by generating a three-dimensional plot of each side chain's distance, angle, and torsion (as defined in Figure 1) as shown in Figure 2. Visual inspection of both the conformational ensembles and the plots obtained for this series of Δ^8-THC analogues suggests that a full and representative sample of conformations was afforded by this technique.

Active Analogue. The results of the conformational volume manipulations are shown in Figure 3. When the common volume of all the conformations of active and inactive analogues was subtracted from the combined volume of all of the conformations of inactive analogues, a spherical region was identified, approximately 8 Å in diameter; this was earlier defined as the AEA. This region is that which is not occupied by conformations of active analogues and is similar to the "receptor essential volume" that is obtained when this approach is applied to single conformations,[38] not conformational ensembles as was done in this instance. A slightly different approach was also utilized wherein the common volume of all active and inactive molecules' conformations was subtracted from the common volume of

Table 3. Comparison of QSAR Models Derived with Real or Random Data

		r^2 values[a]			
		real data		random data	
statistical sampling technique to determine training set composition	activity	cross	final	cross	final
technique 1: 50 random conformations selected from 155 total conformations	pK_D	0.576	0.654	0.384	0.490
	pSA	0.709	0.748	0.317	0.431
	pTF	0.624	0.679	0.366	0.474
	pRT	0.659	0.648	0.315	0.453
technique 2: 10 random conformations selected from 155 total conformations	pK_D	0.411	0.733	0.003	0.576
	pSA	0.518	0.729	0.054	0.527
	pTF	0.441	0.704	0.243	0.599
	pRT	0.479	0.721	0.297	0.496
technique 3: 20 lowest-energy conformations	pK_D	0.650	0.733	0.529	0.652
	pSA	0.722	0.781	0.384	0.560
	pTF	0.691	0.753	0.418	0.592
	pRT	0.693	0.759	0.376	0.501
technique 4: 10 lowest-energy conformations within 50 randomly selected conformations	pK_D	0.586	0.735	0.386	0.602
	pSA	0.690	0.808	0.247	0.596
	pTF	0.642	0.775	0.482	0.676
	pRT	0.681	0.783	0.491	0.670
technique 5: lowest-energy conformation for each analogue	pK_D	−0.248/2	0.653/2	−0.061	0.919
	pSA	0.145/2	0.682/2	−0.141/3	0.775/3
	pTF	0.354/2	0.739/2	−0.463/2	0.553/2
	pRT	0.013/2	0.629/2	−0.291/1	0.179/1

[a] Unless otherwise indicated, the models were derived with five components. If fewer than five components were optimal, the number of components used to derive the model is indicated after the r^2 value.

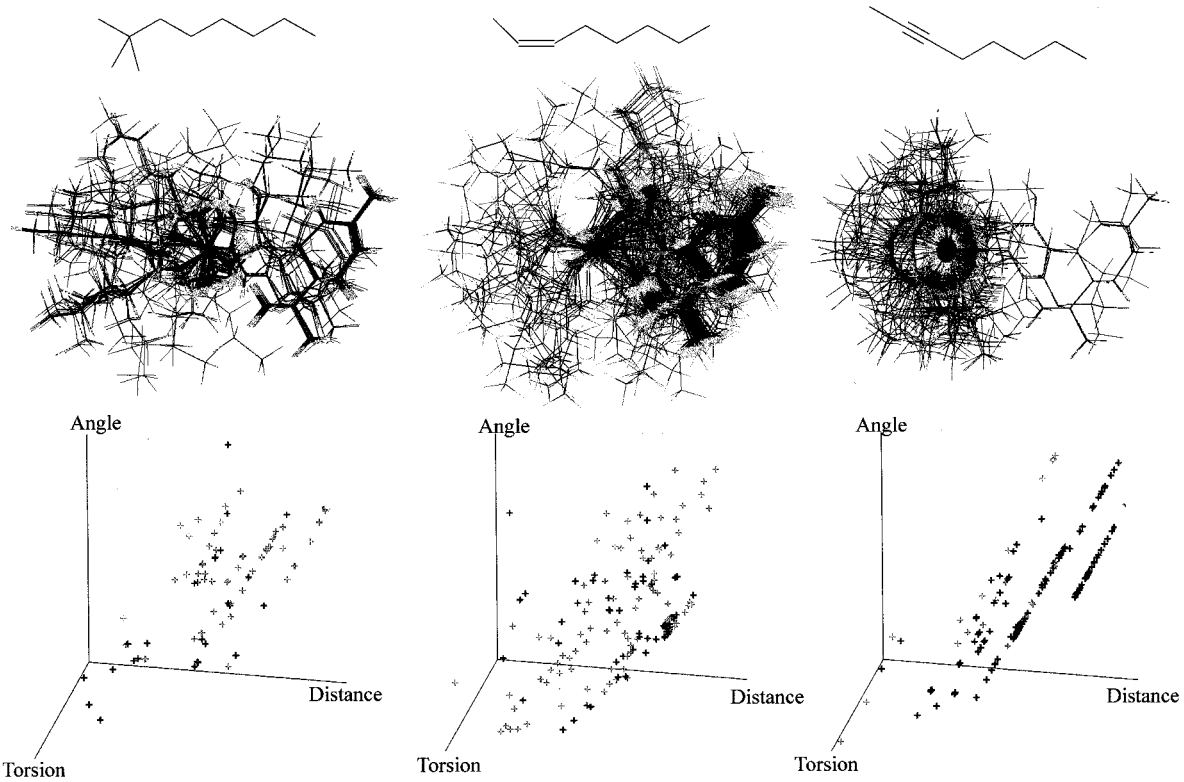

Figure 2. Graphical representations of the conformational ensembles obtained by quenched molecular dynamics for 3-(1,1-dimethylheptyl)-Δ⁸-THC (**36**), left; *cis*-3-(1-heptenyl)-Δ⁸-THC (**2**), middle; and 3-(1-heptynyl)-Δ⁸-THC (**1**), right. For each analogue, a "stick representation" of the side chain is provided at top, an overlay of all 155 conformers is provided in the middle, and a plot of each conformer's side-chain distance, angle, and torsion is provided at the bottom.

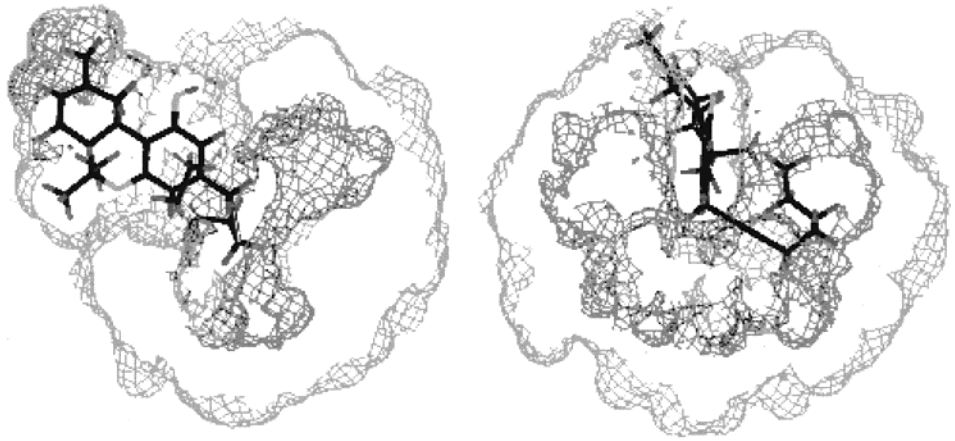

Figure 3. Volumes found in the modified active analogue approach contoured around 3-(3-octynyl)-Δ⁸-THC (**5**). In the left-hand image the ring system is facing the viewer; this is rotated by 90° in the right-hand image, thereby pointing the side chain out of the page. The light gray contour shows the subtraction of the common conformational volume of all active and inactive analogues from the combined conformational volume of only "less active" analogues, revealing the AEA, a unique volume not occupied by conformations of active analogues (larger, outer contour). Contoured in dark gray in the same images is the NR, the volume obtained by subtraction of the common conformational volume of all analogues from the common conformational volume of active analogues, revealing an area that is necessary, albeit not sufficient, for pharmacological affinity and potency within this series of compounds. Note that the AEA (light gray) describes a large surface far from the ring system, indicating that in this region the side chain is extended. The NR (dark gray) wraps both in front of and behind the ring system, as is more visible in the right-hand view, and describes a volume swept out by the more compact conformations of the side chain.

all of the active molecules' conformations; this was earlier identified as the NR. The results of this manipulation of volumes identified a smaller area, contained within the 8 Å sphere, identifying the shared volume of active analogues' conformations that is unique from the volume occupied by both active and inactive analogues. Despite the relatively small number of compounds included in this approach, the results of the volume manipulations were remarkably consistent with the results obtained with the additional SAR analysis techniques described later.

MLR. The explanatory variables of Boltzmann weighted average conformational side-chain distance and angle were correlated to receptor binding affinity as shown in Figure 4. Interestingly, increased length of a compound's side chain (as measured by the distance the end of the side chain was from its ring attachment point) was associated with increased affinity, but the angle of

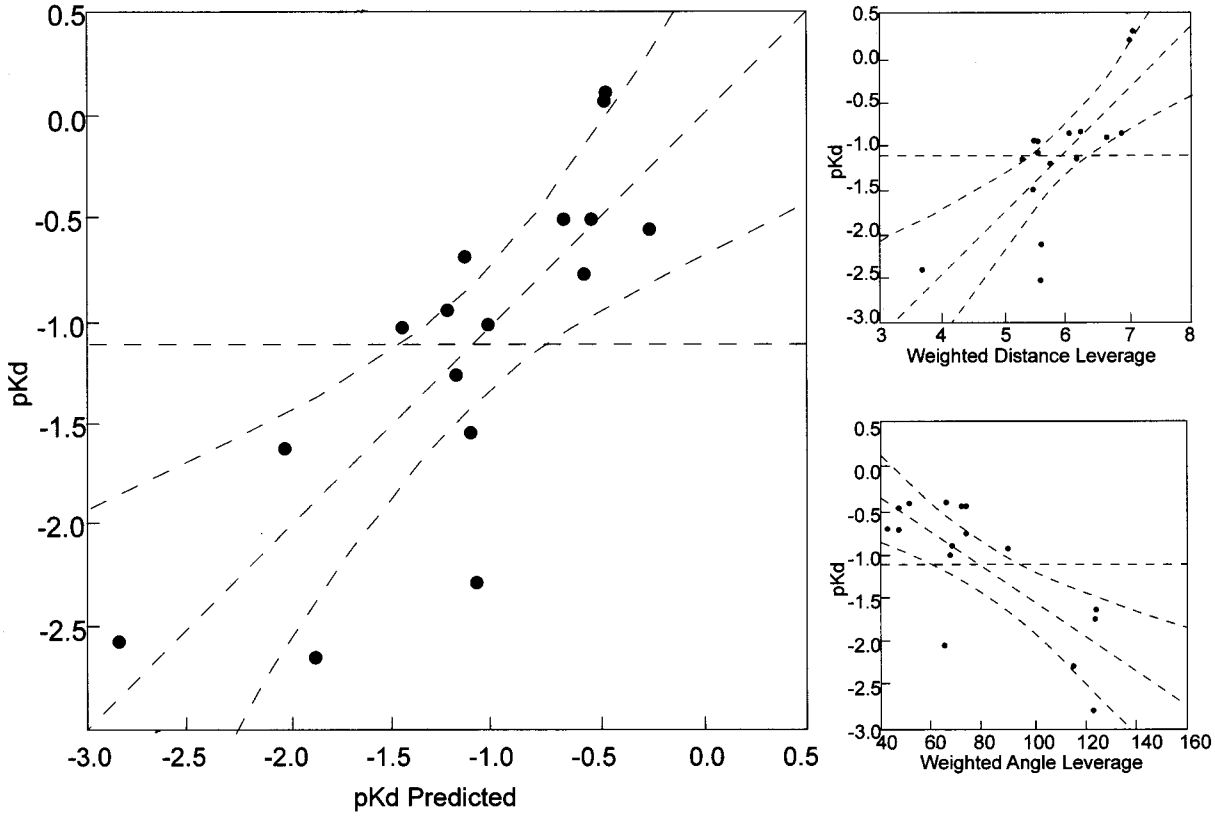

Figure 4. MLR analysis of pK_D using side-chain distance and side-chain angle as independent variables (left). The contribution of the variable describing side-chain distance is shown in the top right plot, and the contribution of the variable describing side-chain angle is shown in the bottom right plot. The dotted lines indicate the linear regression fit and the 95% confidence intervals.

the side chain (as defined in Figure 1) was inversely related to affinity. The torsion angle (see Figure 1) was unable to further contribute to this relationship, and no combination of explanatory variables was able to fit any measure of in vivo pharmacological potency (Table 2). Attempts to extend the MLR analyses to include all of the compounds shown in Table 1 resulted in models that were not able to describe the data with statistical significance (data not shown).

CoMFA. Regardless of the number of conformations used for each analogue or the sampling strategy, the cross-validated analysis of the relationship between the CoMFA molecular fields and the pharmacological affinity and potency measurements generally indicated that a model derived with (the maximum of) five components was optimal. Components are the variables used by SYBYL in developing the QSAR model; five components indicates that five parameters were varied to achieve the predicted data used in the "predicted vs actual" linear regression fit. Note that components do not have a specific physical analogue: they are neither regions of the molecule nor pharmacological assays, but simply a facet of the numerical techniques used to develop a QSAR model. A larger number of components in the equation created to explain activity indicates a more complex and less robust model.

The strength of the cross-validated and final models was demonstrated by comparison with relationships derived with random pharmacological data that spanned the same range as the real pharmacological data. Consistently, the cross-validated or final r^2 values obtained with the real pharmacological data were higher (indicating a better model) than when derived using random pharmacological data (Table 3). For example, when 50 conformations of each of the 36 molecules (1800 conformers total) composed the training set, cross-validated r^2 values of 0.576, 0.709, 0.624, and 0.659 were obtained for the receptor affinity, spontaneous activity, tail-flick, and rectal temperature assays, respectively. These values are considerably higher than those obtained with random data: 0.384, 0.317, 0.366, and 0.315 for receptor affinity, spontaneous activity, tail-flick, and rectal temperature assays, respectively. The final analysis (based on all 1800 conformers being included in the training set) resulted in r^2 values of 0.654, 0.748, 0.679, and 0.648 with real data and 0.490, 0.431, 0.474, and 0.453 for random data (in models derived for receptor affinity, spontaneous activity, tail-flick, and rectal temperature assays, respectively). Whatever sampling technique was used for selecting compounds to compose the training set, there was not a single instance of a model derived with random data possessing a higher r^2 value than a model derived with the actual pharmacological data. Finally, an indication of the influence of the number of components involved in a particular model on the statistical parameters of the fit is provided in Table 4. One can see from this table that despite the increased complexity of the model that occurs by increasing the number of components, the SAR model is statistically strongest when five components are used.

Visualization of CoMFA Fields. Three-dimensional contour plots of the CoMFA model allow the visualization of regions where changes in steric or electrostatic properties are correlated with experimentally determined differences in biological properties. The contour plots in Figure 5 display the QSAR model for both

Table 4. Statistics Obtained with CoMFA/PLS Model for pED_{50}[a]

	number of components				
	1	2	3	4	5
	Cross-Validated Model				
standard error	0.987	0.914	0.875	0.833	0.813
r^2	0.123	0.250	0.316	0.380	0.411
F-value	10.187	24.323	33.565	44.668	50.865
	Final Model				
standard error					0.548
r^2					0.733
F-value					199.7

[a] Model derived from a training set composed of 10 conformations randomly selected for each of the 36 Δ8-THC analogues shown in Table 1.

receptor affinity (top) and pharmacological potency (bottom) in the spontaneous activity assay when derived from a training set of 1800 conformers (50 random conformations from each of 36 molecules). Some of the most heavily weighted regions in the model are depicted in the contour plot at the 90/10 level. However, a view of the same model contoured at the 80/20 level is also provided to reveal additional regions that do not contribute to the model's accuracy as substantively as the 90/10 regions.

Inspection of the steric contour plots reveals a relatively consistent side-chain SAR for both receptor affinity and behavioral potency. In the 80/20 contribution plot, a large contour in yellow surrounds a smaller contour in green in the side-chain region of the analogues. The green contour, in most of the models, actually starts on one side of the aromatic ring and wraps around the side-chain end of the molecule at approximately the level of the C3′ atom until ending near the opposite face of the aromatic ring. This can be more readily seen in the 90/10 contribution plots, where two green contours are visible in this region, one on each side of the ring system. Thus, the model predicts decreased affinity and potency for molecules whose side chains prefer an extended conformation (e.g. an angle of 180° as defined in Figure 1). Alternatively, analogues whose conformational mobility allows their side chain to bend back around in a U-shape, so that the terminus is alongside the aromatic ring, are associated with increased predicted affinity and potency.

The electrostatic plots are best discussed in their spatial relation to prominent regions in the steric plot. For example, in the same regions contoured green in the steric plots, one can see regions contoured blue in several of the electrostatic plots. These blue contours indicate that compounds with positive charge density in this region would be predicted to possess increased pharmacological activity. The regions contoured in red (indicative of where negative charge is associated with increased pharmacological activity) are more widely distributed than the regions in blue and generally correspond to the regions contoured in yellow in the steric plots. Therefore, the model indicates that the worst case scenario for a compound's predicted affinity and potency would be side chains that extend away from the tricyclic ring system and possess positive charges at or near the terminus. Alternatively, the model would predict that the most potent compounds would have long side chains that wrap around to come in close proximity with the ring system and that have positive charge density at the initial side-chain carbons (i.e. in the region of C1′ to C4′).

Discussion

The side chains of all of the analogues in Table 1 are quite flexible, which can make adequate sampling of their conformational mobility and conformationally accessible space difficult. The high-temperature quenched molecular dynamics approach used here has been successfully used in previous studies with anandamide (an arachidonylethanolamide)[24] and arachidonic acid.[39] Furthermore, good agreement has been obtained between quenched molecular dynamics studies and NMR experiments.[40] The apparent completeness of the conformational sampling suggested by visual inspection (Figure 3), the uniform use of this technique for each analogue, and the consistent results of the QSAR analyses (described below) provide further indication of the appropriateness of the conformational sampling techniques.

The active analogue and CoMFA approaches are typically applied to single conformations selected for each analogue and usually involve the identification of a bioactive conformer or the selection of a putative bioactive conformation. However, since the bioactive conformation of the side chain is unknown for cannabinoids, our study used these approaches on conformational ensembles, with no investigator bias involved in the selection of conformations. The use of several conformations for each analogue in a CoMFA study has been tested in a series of styrene derivatives that inhibit protein tyrosine kinase. In that study, it was found that allowing multiple conformers for each compound in the data set yielded improved cross-validated and final r^2 values.[41]

Although investigator bias in the selection of a single conformation was eliminated, the data and results achieved during the QSAR studies are dependent on the molecular alignment system used to compare analogues. We chose to align molecules by overlaying their aromatic rings using a root-mean-square minimization procedure, thereby maximizing the training set's structural differences in the hydrophobic side-chain region and minimizing differences in the ring system. This alignment strategy is arguably the most appropriate, because the two-dimensional structure of the compounds differed only in the side-chain region. Furthermore, the three-dimensional conformational mobility of these analogues also differed primarily in the side-chain region.

The three techniques describe a consistent SAR for the side-chain region of the Δ8-THC analogues. Although there are fine differences between analysis methods, sampling methods (within the CoMFA studies), and pharmacological assays, the overall picture developed is consistent. The results uniformly demonstrate that the side chain's ability to wrap around (in front of and/or behind) the phenol ring system is associated with high affinity and potency. It is in some ways easiest to visualize why this might be the case in the conceptual framework of the simplest approach, the modified active analogue approach. This framework allows us to examine the differences that result from changing the bond order of one bond in the side chain in pairs of otherwise identical alkene/alkyne molecules.

Structure-Activity Derived for
Spontaneous Activity
Assay (ED_{50})
Electrostatic
Steric
Structure-Activity Derived for
CB1 Receptor Binding
Affinity(K_b)
Electrostatic
Steric
80/20
90/10

Let us examine, for example, the 3-(1-heptynyl)- and *cis*-3-(1-heptenyl)-Δ⁸-THC analogues (**1** and **2**). The alkene analogue is notably more active, with a K_D of 0.86 nM vs 36 nM for the alkyne analogue and an average ED_{50} for the three rat behavioral assays of 0.11 mg/kg vs 0.89 mg/kg for the alkyne. The alkyne has a side chain constrained by its triple bond into an extended position; if it were to bend back toward the ring system, it would have to start doing so only after the second carbon. This effectively shortens the length of the side chain available to bend back toward the ring system in two ways. First, the side chain is effectively shorter because it starts bending back after the triple bond, at C3′. Second, the distance the side chain needs to reach to have its terminus alongside the ring system is increased, because the first two side-chain carbons extend directly away from the ring system. There is an established SAR that indicates that longer side chains are correlated with more potent cannabinoids.[23,35] Our data not only corresponds well with this SAR but also adds an explanation for why a longer side chain is needed to increase potency.

Although it was only in the MAA approach that pairs of molecules were actually compared, all modeling/SAR studies are, fundamentally, comparisons of differently potent molecules. The MLR analyses compare a series (rather than a set of pairs) of molecules. The independent variables defined in this analysis facilitated the development of a model with which to understand the Δ⁸-THC analogues' SAR. The variables of distance, angle, and torsion angle (as defined in Figure 1) were chosen simply to localize the side-chain terminus in three-dimensional space, as the MAA approach indicated was needed. These variables had the unexpected effect of providing a terminology with which all three modeling techniques could be discussed. In particular, the language of distance and angle was useful in examining the results of the CoMFA studies.

It is interesting to note that in none of the analyses performed did the torsion angle correlate with the pharmacological data. The CoMFA study indicated that side chains can fold back along either side of the aromatic ring system nonpreferentially. As in the MAA approach, the SAR plots for the CoMFA models indicate regions on both sides of the molecule which, if accessible to the side chain, increase predicted affinity/potency. While it may be that the use of conformational ensembles has precluded the QSAR analyses from being able to differentiate and detect a particular side of the molecule that needs to be occupied by the side chain for optimal activity, it is also possible that the receptor site can accommodate the side chain on either side of the molecule. The MLR data for torsion angle was also nonpredictive because our analysis was designed to seek one, not two (or more), optimal conformations. If there was, in fact, a relationship between torsion angle and activity, the results of the MAA and CoMFA studies indicate that there would be two "preferred" conformations conferring activity, and this would have gone undetected by our MLR studies.

The best correlation coefficient found through MLR analyses was for the K_D. While the variables describing side-chain distance and angle are reasonable predictors of binding affinity, they are less accurate in describing pharmacological potency as measured by the three behavioral assays. In previous structure−activity analyses, the dependent variables of receptor affinity and pharmacological potency have been directly related.[23] However, in the current set of compounds, receptor affinity and pharmacological potency are not correlated. For example, 3-(6-bromo-2-hexynyl)-Δ⁸-THC (**9**) possesses a similar affinity for the cannabinoid receptor as does *cis*-3-(6-bromo-2-hexenyl)-Δ⁸-THC (**10**), yet it is at least 40 times less potent in the tail-flick assay, is over 500-fold less potent in producing hypothermia, and is inactive in producing changes in locomotor activity. Thus, it is not surprising that both affinity and potency cannot be fit with the same MLR model, and this indicates that further investigation may identify the physicochemical properties or structural elements differentially affecting affinity and potency. None of our analyses gave a strong indication of what these structural elements might be. It was not possible to extend the MLR analyses to include all of the compounds shown in Table 1. This technique was limited to the hydrocarbon subset because the other compounds had substantial electrostatic differences which could not be described with the purely conformational variables used in the MLR analysis.

In our CoMFA analyses, each behavioral target property (the CB1 binding and the three behavioral assays for potency) is treated separately and a unique CoMFA model is derived. It is therefore possible to generate independent models for affinity and potency; pharmacological measurements such as ED_{50}'s and IC_{50}'s may rely on structural features that are independent of one another. The similarity of the CoMFA plots indicates that either the structural requirements determining affinity and potency are not able to be well-discriminated by the CoMFA approach or that differences in affinity and potency are being determined by considerations other than receptor interaction (e.g. metabolism, biodisposition, etc).

The CoMFA studies, unlike MAA or MLR analyses, allow examination of the electrostatic properties of the SAR in addition to the steric properties. The various

Figure 5. Stereoviews of the QSARs derived for the steric fields (yellow and green contours) and electrostatic fields (blue and red contours) for cannabinoid receptor (CB1) binding affinity (top half of figure) and for cannabinoid-induced changes in spontaneous locomotor activity (bottom half of figure). The QSARs for the other measures of potency (rectal temperature and tail-flick assays) are not depicted because they are very similar to the spontaneous activity model. The steric plots are depicted so that steric bulk should be moved closer to areas contoured in green and farther from regions contoured in yellow in order to increase the target property being contoured (i.e. affinity or potency). The electrostatic plots are contoured such that positive charge should be moved closer to regions contoured in blue and farther from regions contoured in red in order to increase the target property being contoured. For each model, two levels of contribution are depicted, one at an 80/20 level of contribution and one showing the more heavily weighted region of 90/10 contribution (as noted in images). The numbers 90/10 and 80/20 are percentiles of the overall range of values within the CoMFA field. For example, 90 indicates that the regions displayed are those which contribute within the top 10% of positive (green) interaction, and 10 indicates that the regions displayed are those which contribute within the top 10% of negative (yellow) interaction.

PLS analyses all indicate that higher affinity/efficacy correlates with positive charge at the C1′ to C3′ positions of the side chain and negative charge further along the side chain. There are several possible explanations for this. First, some of the most active members of our data set were *cis*-alkene-Δ^8-THC analogues. The π electron cloud of this double bond is a significant source of negative charge, yet it is not necessarily the negative charge which causes increased activity; it may be the steric effects of a cis double bond which begins to bend the side chain back toward the phenyl ring system. It is also possible that the electrostatic effects are due to receptor interactions; this study does not provide sufficient information to comment definitively on these questions.

The steric aspects of the QSAR developed in this work are supported by data from several experimental techniques. For example, in NMR studies of the nonclassical cannabinoid CP-47,497,[42] a folded back conformation of the 1′,1′-dimethylheptyl side chain of CP-47,497 has been demonstrated to be a preferred conformation. The position of the terminus of the side chain relative to the remainder of the molecule was not determined in these studies. However, the side chain was noted to prefer a conformation in which the 3′-CH_2 protons are located above or below the aromatic ring. Thus, our QSAR data are consistent with an NMR-observable preferred conformation of a relatively high potency 1′,1′-dimethylheptyl side-chain-containing cannabinoid analogue. Furthermore, in model membrane systems, neutron diffraction has been used to assess the topography of Δ^8-THC. These studies also indicate a compact conformation is preferred, where the terminus of the pentyl side chain aligns itself at the level of the tricyclic ring system.[43]

It is interesting to note how the results of these QSAR studies apply to the parent molecule of all analogues studied, Δ^8-THC (**16**). Δ^8-THC is relatively less efficacious than many of its analogues studied here, possibly because its side chain is relatively short and is thus unable to wrap around the phenyl ring system as fully as longer side chains. 3-(1′,1′-Dimethylheptyl)-Δ^8-THC (**36**) also has a shorter side chain than many of the analogues studied but is one of the most efficacious analogues examined. This may be a result of the branches on the side chain forcing the side chain into a more compact, or folded, conformation.

Our finding that side chains that can wrap backward along either side of the molecule are associated with fully efficacious, high-affinity ligands might explain the limited success that has been achieved with constrained side-chain analogues. For example, Busch-Petersen et al.[33] synthesized four analogues of β-11-hydroxyhexahydrocannabinol (HHC) varying in the rotational freedom around the first three carbon atoms. Three of the corresponding Δ^8-THC side-chain analogues are contained within our training set: the 3-(1-heptynyl)-Δ^8-THC (**1**), the *cis*-3-(1-heptenyl)-Δ^8-THC (**2**), and the 3-(1′,1′-dimethylheptyl)-Δ^8-THC (**36**). The fourth analogue, the *trans*-3-(1-heptenyl) analogue, was not included in our SAR studies; however, conformational analysis was performed using our quenched molecular dynamics approach (data not shown). The investigators noted that there was not a tremendous separation in the affinities of the 4-β-11-HHC side-chain analogues tested, with the *alkyne analogue possessing the lowest activity*, and suggested that this is in accordance with an existing SAR that indicates that seven-carbon atom side chains in cannabinoids are associated with high affinities and potencies. However, we feel that these compounds share similar affinities because the degree of side-chain constraint imposed is not sufficient to exclude any one analogue from assuming conformations shared with other analogues in this series (Figure 3), including the putative bioactive conformation suggested by our SAR studies.

Chart 1. Ring-Constrained Analogues of Cannabinoids

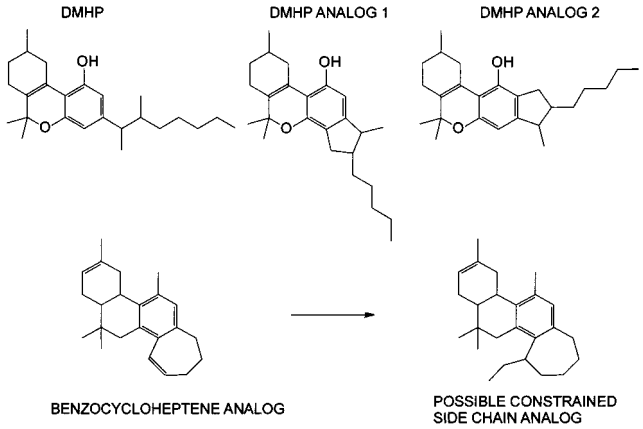

More recently, Papahatjis et al.[31] published a study involving six additional side-chain-constrained analogues of Δ^8-THC, including the 3-(1-heptynyl) analogue synthesized in the aforementioned β-11-HHC series and a potent 1′-dithiolane derivative. The authors noted that no analogue had the side chain in a fully restricted conformation. However, they concluded from their binding data, and in particular the increased potency of the 1′-dithiolane and the 1′-methylene analogues, that a hydrophobic subsite of the cannabinoid pharmacophore exists in both CB1 and CB2 at the level of the benzylic side-chain carbon. We believe it is also possible that the 1′-dithiolane, the 1′-methylene, and even the 1′-keto functional groups might, due to steric interactions, serve to bend the side chain back along the ring system into the bioactive conformation suggested by our CoMFA studies. The decreased affinity of the keto group when compared to the methylene group was interpreted by the authors as indicating the hydrophobic nature of the subsite. However, our CoMFA studies indicate that positively charged substituents in this region would be associated with increased pharmacological potency and receptor affinities (see Figure 5). Thus, as is the case in the 1′-keto analogue, an electronegative atom such as an oxygen atom at the 1′-position would be predicted to lead to decreased affinity and potency in our QSAR model. These results suggest that the region around the 1′-position is not strictly hydrophobic in nature.

Constrained side chains have also been synthesized using ring systems to induce specific orientations of the side chain (Chart 1). For example, cyclic side-chain analogues of the extremely potent dimethylheptylpyran (DMHP) have been synthesized using 2,3- and 3,4-bridged pentyl ring systems.[44] However, the ring-constrained compounds were inactive as CNS and cardiovascular agents in mice and rats. It is possible that this is due to the ring systems' orientation of the

side chain away from the ring system, reducing the side chain's ability to wrap back around the molecule. Unfortunately, there are few conceivable ring-constrained side-chain analogues that can be readily synthesized that would facilitate the side chain being able to tightly wrap around the molecule in close proximity with the tricyclic ring system. This is due to the aromatic nature of the ring system and the unavailability of ring protons at the 1-, 5-, and 6-positions to which the side chain might be wrapped back and attached. However, the benzocycloheptene analogue reported by Seltzman (Chart 1) may provide an appropriate ring system to which further side-chain alkenes can be added at a variety of positions to further explore the side-chain region of the cannabinoid pharmacophore.[45] Unfortunately, this compound has never been tested in cannabinoid pharmacological assays.

Conclusions

The standard conviction regarding cannabinoid side-chain SAR is that extending the side chain up to seven or eight carbons is associated with increased pharmacological potency. However, the region that the side chain must extend into for optimal activity, if any, has not been reported. Using three SAR paradigms with 36 analogues of Δ^8-THC, we have acquired consistent data indicating the pharmacophoric requirements of the side chain not only involve extensions of the side chain away from the point of attachment but must also involve the side chain folding back so that the terminus is in proximity to the ring system. In addition, positive charge in the region occupied by C1′ to C3′ and negative charge further away from the attachment point of the side chain are predicted to result in compounds with increased affinity and potency. While the approaches we utilized involved the use of conformational ensembles, which is relatively unusual in the SAR techniques we employed, the consistent application of the methods, the comparison of the results with randomized data, and the concordant results afforded by all three approaches add support for these newly described pharmacophoric requirements of the side chain. Finally, this pharmacophore model of the side chain appears to be able to fit the pharmacological data of a wide variety of analogues and to aide in the explanation of the activity or inactivity of previously synthesized side-chain-constrained analogues.

Acknowledgment. This work was supported by a National Institute on Drug Abuse grant (DA11638).

Supporting Information Available: Pharmacological data for Δ^8-THC side-chain analogues. This material is available free of charge via the Internet at http://pubs.acs.org.

References

(1) Devane, W. A.; Dysarz, F. A.; Johnson, M. R.; Melvin, L. S.; Howlett, A. C. Determination and characterization of a cannabinoid receptor in rat brain. *Mol. Pharmacol.* **1988**, *34*, 605−613.
(2) Munro, S.; Thomas, K. L.; Abu-Shaar, M. Molecular characterization of a peripheral receptor for cannabinoids. *Nature* **1993**, *365*, 61−65.
(3) Howlett, A. C.; Johnson, M. R.; Melvin, L. S.; Milne, G. M. Nonclassical cannabinoid analgetics inhibit adenylate cyclase: development of a cannabinoid receptor model. *Mol. Pharmacol.* **1988**, *33*, 297−302.
(4) Matsuda, L. A.; Lolait, S. J.; Brownstein, M. J.; Young, A. C.; Bonner, T. I. Structure of a cannabinoid receptor and functional expression of the cloned cDNA. *Nature* **1990**, *346*, 561−564.
(5) Deadwyler, S. A.; Hampson, R. E.; Mu, J.; Whyte, A.; Childers, S. Cannabinoids modulate voltage sensitive potassium A-current in hippocampal neurons via a cAMP-dependent process. *J. Pharmacol. Exp. Ther.* **1995**, *273*, 734−743.
(6) Mackie, K.; Hille, B. Cannabinoids inhibit N-type calcium channels in neuroblastoma-glioma cells. *Proc. Natl. Acad. Sci. U.S.A.* **1992**, *89*, 3825−3829.
(7) Mackie, K.; Lai, Y.; Westenbroek, R.; Mitchell, R. Cannabinoids activate an inwardly rectifying potassium conductance and inhibit Q-type calcium currents in AtT20 cells transfected with rat brain cannabinoid receptor. *J. Neurosci.* **1995**, *15*, 6552−6561.
(8) Compton, D. R.; Rice, K. C.; De Costa, B. R.; Razdan, R. K.; Melvin, L. S.; Johnson, M. R.; Martin, B. R. Cannabinoid structure−activity relationships: correlation of receptor binding and in vivo activities. *J. Pharmacol. Exp. Ther.* **1993**, *265*, 218−226.
(9) Razdan, R. K. Structure−activity relationships in cannabinoids. *Pharmacol. Rev.* **1986**, *38*, 75−149.
(10) Compton, D. R.; Aceto, M. D.; Lowe, J.; Martin, B. R. In vivo characterization of a specific cannabinoid receptor antagonist (SR141716A): inhibition of delta 9-tetrahydrocannabinol-induced responses and apparent agonist activity. *J. Pharmacol. Exp. Ther.* **1996**, *277*, 586−594.
(11) Mansbach, R. S.; Rovetti, C. C.; Winston, E. N.; Lowe, J. A. Effects of the cannabinoid CB1 receptor antagonist SR141716A on the behavior of pigeons and rats. *Psychopharmacology (Berlin)* **1996**, *124*, 315−322.
(12) Herkenham, M.; Lynn, A. B.; Little, M. D.; Johnson, M. R.; Melvin, L. S.; de Costa, B. R.; Rice, K. C. Cannabinoid receptor localization in brain. *Proc. Natl. Acad. Sci. U.S.A.* **1990**, *87*, 1932−1936.
(13) Jansen, E. M.; Haycock, D. A.; Ward, S. J.; Seybold, V. S. Distribution of cannabinoid receptors in rat brain determined with aminoalkylindoles. *Brain Res.* **1992**, *575*, 93−102.
(14) Felder, C. C.; Joyce, K. E.; Briley, E. M.; Glass, M.; Mackie, K. P.; Fahey, K. J.; Cullinan, G. J.; Hunden, D. C.; Johnson, D. W.; Chaney, M. O.; Koppel, G. A.; Brownstein, M. LY320135, a novel cannabinoid CB1 receptor antagonist, unmasks coupling of the CB1 receptor to stimulation of cAMP accumulation. *J. Pharmacol. Exp. Ther.* **1998**, *284*, 291−297.
(15) Devane, W. A.; Hanus, L.; Breuer, A.; Pertwee, R. G.; Stevenson, L. A.; Griffin, G.; Gibson, D.; Mandelbaum, A.; Etinger, A.; Mechoulam, R. Isolation and structure of a brain constituent that binds to the cannabinoid receptor. *Science* **1992**, *258*, 1946−1949.
(16) Rinaldi-Carmona, M.; Barth, F.; Heaulme, M.; Shire, D.; Calandra, B.; Congy, C.; Martinez, S.; Maruani, J.; Neliat, G.; Caput, D.; et al. SR141716A, a potent and selective antagonist of the brain cannabinoid receptor. *FEBS Lett.* **1994**, *350*, 240−244.
(17) Shire, D.; Calandra, B.; Delpech, M.; Dumont, X.; Kaghad, M.; Le Fur, G.; Caput, D.; Ferrara, P. Structural features of the central cannabinoid CB1 receptor involved in the binding of the specific CB1 antagonist SR 141716A. *J. Biol. Chem.* **1996**, *271*, 6941−6946.
(18) Reggio, P. H.; McGaughey, G. B.; Odear, D. F.; Seltzman, H. H.; Compton, D. R.; Martin, B. R. A rational search for the separation of psychoactivity and analgesia in cannabinoids. *Pharmacol. Biochem. Behav.* **1991**, *40*, 479−486.
(19) Reggio, P. H.; Panu, A. M.; Miles, S. Characterization of a region of steric interference at the cannabinoid receptor using the active analogue approach. *J. Med. Chem.* **1993**, *36*, 1761−1771.
(20) Reggio, P. H.; Bramblett, R. D.; Yuknavich, H.; Seltzman, H. H.; Fleming, D. N.; Fernando, S. R.; Stevenson, L. A.; Pertwee, R. G. The design, synthesis and testing of desoxy-CBD: further evidence for a region of steric interference at the cannabinoid receptor. *Life Sci.* **1995**, *56*, 2025−2032.
(21) Semus, S. F.; Martin, B. R. A computergraphic investigation into the pharmacological role of the THC-cannabinoid phenolic moiety. *Life Sci.* **1990**, *46*, 1781−1785.
(22) Shim, J. Y.; Collantes, E. R.; Welsh, W. J.; Subramaniam, B.; Howlett, A. C.; Eissenstat, M. A.; Ward, S. J. Three-dimensional quantitative structure−activity relationship study of the cannabimimetic (Aminoalkyl)indoles using comparative molecular field analysis. *J. Med. Chem.* **1998**, *41*, 4521−4532.
(23) Thomas, B. F.; Compton, D. R.; Martin, B. R.; Semus, S. F. Modeling the cannabinoid receptor: a three-dimensional quantitative structure−activity analysis. *Mol. Pharmacol.* **1991**, *40*, 656−665.
(24) Thomas, B. F.; Adams, I. B.; Mascarella, S. W.; Martin, B. R.; Razdan, R. K. Structure−activity analysis of anandamide analogues: relationship to a cannabinoid pharmacophore. *J. Med. Chem.* **1996**, *39*, 471−479.
(25) Tong, W.; Collantes, E. R.; Welsh, W. J.; Berglund, B. A.; Howlett, A. C. Derivation of a pharmacophore model for an-

andamide using constrained conformational searching and comparative molecular field analysis. *J. Med. Chem.* **1998**, *41*, 4207−4215.
(26) Xie, X. Q.; Eissenstat, M.; Makriyannis, A. Common cannabimimetic pharmacophoric requirements between aminoalkyl indoles and classical cannabinoids. *Life Sci.* **1995**, *56*, 1963−1970.
(27) Martin, B. R.; Compton, D. R.; Semus, S. F.; Lin, S.; Marciniak, G.; Grzybowska, J.; Charalambous, A.; Makriyannis, A. Pharmacological evaluation of iodo and nitro analogues of delta 8-THC and delta 9-THC. *Pharmacol. Biochem. Behav.* **1993**, *46*, 295−301.
(28) Adams, R. Marijuana. *Harvey Lectures* **1942**, *37*, 168−197.
(29) Winn, M.; Arendsen, D.; Dodge, P.; Dren, A.; Dunnigan, D.; Hallas, R.; Hwang, K.; Kyncl, J.; Lee, Y. H.; Plotnikoff, N.; Young, P.; Zaugg, H. Drugs derived from cannabinoids. 5. delta-6a,10a-Tetrahydrocannabinol and heterocyclic analogues containing aromatic side chains. *J. Med. Chem.* **1976**, *19*, 461−471.
(30) Martin, B. R.; Kallman, M. J.; Kaempf, G. F.; Harris, L. S.; Dewey, W. L.; Razdan, R. K. Pharmacological potency of R- and S-3′-hydroxy-delta9-tetrahydrocannabinol: additional structural requirement for cannabinoid activity. *Pharmacol. Biochem. Behav.* **1984**, *21*, 61−65.
(31) Papahatjis, D. P.; Kourouli, T.; Abadji, V.; Goutopoulos, A.; Makriyannis, A. Pharmacophoric requirements for cannabinoid side chains: multiple bond and C1′-substituted delta 8-tetrahydrocannabinols. *J. Med. Chem.* **1998**, *41*, 1195−1200.
(32) Martin, B. R.; Compton, D. R.; Prescott, W. R.; Barrett, R. L.; Razdan, R. K. Pharmacological evaluation of dimethylheptyl analogues of delta 9-THC: reassessment of the putative three-point cannabinoid-receptor interaction. *Drug Alcohol Depend.* **1995**, *37*, 231−240.
(33) Busch-Petersen, J.; Hill, W. A.; Fan, P.; Khanolkar, A.; Xie, X. Q.; Tius, M. A.; Makriyannis, A. Unsaturated side chain beta-11-hydroxyhexahydrocannabinol analogues. *J. Med. Chem.* **1996**, *39*, 3790−3796.
(34) Martin, B. R.; Compton, D. R.; Thomas, B. F.; Prescott, W. R.; Little, P. J.; Razdan, R. K.; Johnson, M. R.; Melvin, L. S.; Mechoulam, R.; Ward, S. J. Behavioral, biochemical, and molecular modeling evaluations of cannabinoid analogues. *Pharmacol. Biochem. Behav.* **1991**, *40*, 471−478.
(35) Schmetzer, S.; Greenidge, P.; Kovar, K. A.; Schulze-Alexandru, M.; Folkers, G. Structure−activity relationships of cannabinoids: a joint CoMFA and pseudoreceptor modelling study. *J. Comput.-Aided Mol. Des.* **1997**, *11*, 278−292.
(36) Nicklaus, M. C.; Wang, S.; Driscoll, J. S.; Milne, G. W. Conformational changes of small molecules binding to proteins. *Bioorg. Med. Chem.* **1995**, *3*, 411−428.
(37) Martin, B. R.; Jefferson, R.; Winckler, R.; Wiley: J. L.; Huffman, J. W.; Crocker, P. J.; Saha, B.; Razdan, R. K. Manipulation of the tetrahydrocannabinol side chain delineates agonists, partial agonists, and antagonists. *J. Pharmacol. Exp. Ther.* **1999**, *290*, 1065−1079.
(38) Marshall, G. R.; Barry, C. D.; Bosshard, H. E.; Dammkoehler, R. A.; Dunn, D. A. The Conformational Parameter in Drug Design: The Active Analogue Approach. In *Computer-Assisted Drug Design*; Olson, E. C., Christoffersen, R. E., Eds.; American Chemical Society: Washington, DC, 1979; p 619.
(39) Rich, M. R. Conformational analysis of arachidonic and related fatty acids using molecular dynamics simulations. *Biochim. Biophys. Acta* **1993**, *1178*, 87−96.
(40) Altomare, C.; Cellamare, S.; Carotti, A.; Casini, G.; Ferappi, M.; Gavuzzo, E.; Mazza, F.; Carrupt, P. T.; Gaillard, P.; Testa, B. X-ray crystal structure, partitioning behavior, and molecular modeling study of piracetam-type nootropics: insights into the pharmacophore. *J. Med. Chem.* **1995**, *38*, 170−179.
(41) Nicklaus, M. C.; Milne, G. W.; Burke, T. R., Jr. QSAR of conformationally flexible molecules: comparative molecular field analysis of protein-tyrosine kinase inhibitors. *J. Comput.-Aided Mol. Des.* **1992**, *6*, 487−504.
(42) Xie, X. Q.; Yang, D. P.; Melvin, L. S.; Makriyannis, A. Conformational analysis of the prototype nonclassical cannabinoid CP-47,497, using 2D NMR and computer molecular modeling. *J. Med. Chem.* **1994**, *37*, 1418−1426.
(43) Martel, P.; Makriyannis, A.; Mavromoustakos, T.; Kelly, K.; Jeffrey, K. R. Topography of tetrahydrocannabinol in model membranes using neutron diffraction. *Biochim. Biophys. Acta* **1993**, *1151*, 51−58.
(44) Razdan, R. K.; Haldean, C. D. Drugs derived from cannabinoids. 6. Synthesis of Cyclic analogues of dimethylheptylpyran. *J. Med. Chem.* **1976**, *19*, 719−721.
(45) Seltzman, H. H.; Setzer, S. R.; Williams, D. L.; Demian, I.; Wyrick, C.; Pitt, C. G. Syntheses of cannabinoid radioligands and haptens for use in radioimmunoassay and receptor site studies. In *Marihuana 84: Proceedings of the Oxford Symposium on Cannabis;* Harvey, D. J., Ed.; IRL Press: Oxford, England, 1984; pp 183−189.

JM9902281